Apparent Viscosity of a Fluid–Gas Mixture

DAVID H. LEWIS, JR., and P. R. RYASON,* *Jet Propulsion Laboratory, California Institute of Technology, Pasadena, California 91103*

Synopsis

The inertia free flow of a one-dimensional, isothermal fluid–gas mixture in a tube of constant radius is analyzed. The fluid is viscous, non-Newtonian, and incompressible; the gas is inviscid and compressible. Integration of the equations of continuity, momentum, and state enable the prediction of axial pressure, velocity, density, volumetric flow rate, and shear–stress profiles. Departures from corresponding profiles observed in the flow of non-Newtonian power-law fluids are evident. The apparent viscosity of the fluid–gas mixture is computed and compared to that of the fluid alone. A reduction in apparent viscosity is noted. Previously reported experimental evidence of a reduction in viscosity in a non-Newtonian fluid–gas mixture is recalled and it is claimed that the physical model presented here is capable of explaining the observed reduction in apparent viscosity.

INTRODUCTION

Fluid–gas mixtures represent a fluid mechanical problem of current technological interest. Flows of this type occur throughout the foam processing industry, in extruders and dies, for example. Previously, both theoretical[3] and experimental[1–3] studies have been conducted to investigate specific aspects of these flows. Blyer and Kwei[1] present a free-volume viscosity model to account for the experimental observation that when small amounts of gas are added to a non-Newtonian power-law fluid the apparent viscosity of the resulting fluid–gas mixture decreases. An understanding of this phenomena would be an aid in the rational design of foam manufacturing equipment. In this article, a physical model of a fluid–gas mixture is presented and the apparent viscosity of the mixture is computed. This result is compared to the viscosity of the fluid alone, and a reduction in apparent viscosity is observed. This reduction in apparent viscosity is consistent with previously reported experiments using non-Newtonian fluid–gas mixtures.

MATHEMATICAL MODEL

In the following analysis, we are concerned with the one-dimensional, isothermal flow of a viscous fluid containing homogeneously dispersed bubbles of gas. Application of mass and momentum conservation and the equation-of-state of the fluid–gas mixture enables the reduction of axial pressure, velocity, density, volumetric flow rate, and shear–stress profiles.

The fluid is considered non-Newtonian and incompressible. The fluid density, ρ_f, is assumed constant and the fluid viscosity, η_f, is assumed to obey a power-law relationship with shear rate, $\eta_f = m\dot{\gamma}^{n-1}$.[1,2] The constants m and n are parameters characterizing the fluid, and $\dot{\gamma}$ is the shear rate. The gas is considered

* Present Address: Chevron Research Company, Richmond, California.

Journal of Applied Polymer Science, Vol. 25, 1695–1702 (1980)
© 1980 John Wiley & Sons, Inc.
0021-8995/80/0025-1695$01.00

inviscid and obeys the equation of state $p = \rho_g \mathcal{R} T$, where p is the pressure, ρ_g the gas density, $\mathcal{R}$ the specific gas constant, and T the temperature of the gas. Furthermore, it is assumed that the gas is insoluble in the fluid, and the gas temperature is constant and equal to the fluid temperature. The ratio of the mass of gas to the mass of fluid, denoted r, is assumed constant and is defined as $r = M_g/M_f$. The density of the fluid–gas continuum is defined as $\rho = M/V$; where ρ is the density of the mixture, M the total mass of the mixture, and V the total volume. Substituting for the fluid and gas contributions to M and V and introducing the gas equation of state yields the equation of state of the fluid–gas mixture.

$$\rho = \frac{M}{V} = \frac{\rho_f V_f + \rho_g V_g}{V_f + V_g} = \frac{\rho_f V_f (1 + \rho_g V_g/\rho_f V_f)}{V_f + V_g} = \frac{p\rho_f (1 + r)}{(p_r + p)} \tag{1}$$

where $p_r = r\rho_f \mathcal{R} T$ has been introduced for convenience. This model requires that the gas and fluid phases be at the same pressure, thus surface tension effects are neglected.

To complete the mathematical formulation of the problem, we not apply the principle of mass and momentum conservation to the one-dimensional tube of radius R shown in Figure 1.

Conservation of mass

$$\rho u = G = \text{constant} \tag{2}$$

Conservation of momentum

$$-\pi R^2 dp - \tau_w 2\pi R dx (A_f/A) = \pi R^2 d(\rho u^2) \tag{3}$$

In Eq. (3) τ_w is the wall shear stress and A_f is the area wetted by the fluid. This model assumes that the shear stress is transmitted by the fluid alone, hence the introduction of A_f. The area A_f can be related to the tube area A as follows:

$$A = A_f + A_g = A_f(1 + A_g/A_f) = A_f(1 + \epsilon) \tag{4}$$

The area wetted by the gas A_g and ϵ = gas volume/fluid volume = $r\rho_f \mathcal{R} T/p = p_r/p$ have been introduced in eq. (4).

It is now necessary to relate the wall shear stress, τ_w, to the fluid–gas mixture velocity u so that an integration of the equation of motion can be performed. We adopt a friction-factor type of correlation, namely

$$\tau_w = \tfrac{1}{2} \rho u^2 f \tag{5}$$

In many non-Newtonian fluids at low Reynolds number, the friction factor f is

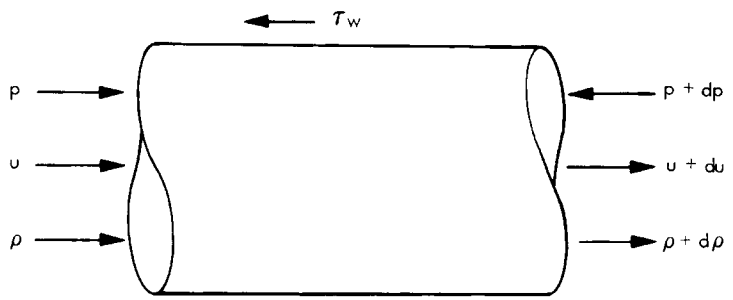

Fig. 1. Schematic diagram of one-dimensional steamtube.

correlated with Reynolds number by $f = 16/\mathrm{Re}$, where $\mathrm{Re} = 8u^{2-n}\rho R^n/m(3 + 1/n)^n$.[2,4–6]

We assume here that the viscosity is high enough and the length scale small enough so that the flow is inertia-free and the friction factor representation is valid. The Reynolds number is the value based on the flow properties averaged over the tube cross section. This is consistent with the assumption that the fluid alone contributes to the wall shear stress.

Combining eqs. (1)–(5) and eliminating u yields the following differential equation for pressure:

$$-dp - \frac{2m\,(5G)^{1/2}}{R^{3/2}\,[(1 + r)\rho_f]^{1/2}}\frac{p^{1/2}}{(p_r + p)^{1/2}}\,dx = \frac{-G^2 p_r}{(1 + r)\rho_f p^2}\,dp \tag{6}$$

In eq. (6) the parameter n has been given the value $n = \frac{1}{2}$, a typical value for polyethylene plastics.

The following nondimensional variables, denoted by superscript*, are introduced:

$$p^* = p/p_0$$

$$\rho^* = \rho/\rho_f$$

$$x^* = x/L$$

$$p_r^* = p_r/p_0$$

where p_0 and L are the reservoir pressure and capillary length, respectively.

Equation (6) can be written in dimensionless terms as:

$$-dp^* - \frac{2mL\,(5G)^{1/2}\,p^{*1/2}}{p_0 R^{3/2}\,[(1 + r)\rho_f]^{1/2}\,(p_r^* + p^*)^{1/2}}\,dx^* = \frac{-G^2 p_r^*}{(1 + r)\rho_f p_0 p^{*2}}\,dp^* \tag{7}$$

subject to the boundary conditions; $p^*(x^* = 0) = 1$ and $p^*(x^* = 1) = p_a/p_0$ where p_a is the downstream pressure. Since eq. (7) is a first-order differential equation with two boundary conditions, G is an eigenvalue in this problem. This is reasonable, since for an imposed pressure drop, the mass flow rate is determined for a given fluid–gas mixture and this is the eigenvalue G.

RESULTS

As a representative example, we have chosen the following values for the constants that appear explicitly and implicitly in eq. (7); $p_0 = 100$ atm $= 1.014\ 10^8$ dyn/cm^2, p_a = downstream pressure = 1 atm $= 1.014\ 10^6$ dyn/cm^2, $\rho_f = 0.7585$ g/cm^3, $L = 2.54$ cm, $R = 0.023$ cm, $r = 0.005$, $m = 7.22\ 10^4$ dyn sec$^{1/2}$/cm^2, $n = \frac{1}{2}$, $T = 200$°C, $\mathcal{R} = 4.514$ cal/gK, $p_r = r\rho_f \mathcal{R} T = 6.692$ atm $= 6.7857\ 10^6$ dyn/cm^2, $p_r^* = p_r/p_0 = 0.06692$. These values are typical of those found in the flows of low-density polyethylene (LDPE) plastics in capillary rheometers.

The inertia-free form of eq. (7) can be integrated numerically with the proper choice of G. For $G = 0.17718$ g m/cm^2 sec, the resulting pressure profile matches the required boundary conditions of $p^*(x^* = 0) = 1$ and $p^*(x^* = 1) = p_a/p_0 = 1/100 = 0.01$ to an accuracy of 0.01%. The dimensionless pressure profile is tabulated in Table I and shown graphically in Figure 2. From G, $u_o \equiv u(x = 0)$ can be determined as $u_0 = G/\rho(x = 0) = 0.17718/0.7145 = 0.2480$ cm/sec. The profiles of dimensionless velocity, $u^* = u/u_0$, and density $\rho^* = \rho/\rho_f$, can be de-

TABLE I
Values of p^*, ρ^*, u^*, τ^*_{weff} vs. x^*

x^*	$p^* = \frac{p}{p_0}$	$\rho^* = \frac{\rho}{\rho_f} = \frac{(1+r)p^*}{p_r^* + p^*}$	$u^* = \frac{\rho_0^*}{\rho^*}$	τ^*_{weff}[a]
0.00	1.0000	0.9420	1.000	1.000
0.04	0.9567	0.9393	1.003	0.9987
0.08	0.9135	0.9364	1.006	0.9971
0.12	0.8704	0.9332	1.009	0.9951
0.16	0.8274	0.9298	1.013	0.9935
0.20	0.7844	0.9260	1.017	0.9914
0.24	0.7415	0.9218	1.022	0.9893
0.28	0.1988	0.9172	1.027	0.9868
0.32	0.6561	0.9120	1.033	0.9840
0.36	0.6136	0.9062	1.040	0.9811
0.40	0.5712	0.8996	1.047	0.9772
0.44	0.5290	0.8921	1.056	0.9732
0.48	0.4869	0.8836	1.066	0.9685
0.52	0.4451	0.8736	1.078	0.9629
0.56	0.4036	0.8621	1.093	0.9568
0.60	0.3623	0.8403	1.110	0.9488
0.64	0.3214	0.8318	1.132	0.9395
0.68	0.2810	0.8117	1.160	0.9281
0.72	0.2411	0.7866	1.198	0.9140
0.76	0.2019	0.7548	1.248	0.8952
0.80	0.1637	0.7134	1.320	0.8701
0.84	0.1267	0.6576	1.432	0.8354
0.88	0.0916	0.5807	1.622	0.7851
0.92	0.0591	0.4713	1.999	0.7074
0.94	0.0444	0.4008	2.350	0.6523
0.96	0.0310	0.3182	2.960	0.5812
0.98	0.0194	0.2259	4.170	0.4897
1.00	0.01	0.1306	7.213	0.3724

[a] $\tau^*_{weff} = \dfrac{\tau_{weff}(x)}{\tau_{weff}(x=0)} = u^{*1/2}\dfrac{p^*(1+p^*)}{p^* + p_r^*}$.

termined from the continuity and state equations, respectively. These results are presented in Table I and in Figures 3 and 4. The effective wall shear stress, $\tau_{weff}(x) = \tau_w(x)/1 + \epsilon(x) = m(5u)^{1/2}/R^{1/2}[1 + \epsilon(x)]$, is shown in Figure 5 and in Table I, nondimensionalized by $\tau_{w0eff} = \tau_w(x = 0)/1 + \epsilon(x = 0)$ as $\tau^*_{weff} = \tau_{weff}(x)/\tau_{w0eff} = u^{*1/2}p^*(p_r^* + 1)/(p_r^* + p^*)$. In forming τ^*_{weff}, the result $\epsilon(x) = p_r/p$ has been used. The volumetric flow rate, $Q = u\pi R^2$, is shown in Figure 3 as $Q^* = Q(x)/Q(x = 0)$; clearly $u^* = Q^*$. The length-averaged effective wall shear stress $\bar{\tau}_{weff}$ is a useful quantity; it is

$$\bar{\tau}_{weff} = \frac{1}{L}\int_0^L \tau_{weff}(x)\,dx = \tau_{w0eff}\int_0^1 \tau^*_{weff}\,dx^*$$

$$= \frac{m(5u_0)^{1/2}}{R^{1/2}[1 + \epsilon(x=0)]^0}\int_0^1 \tau^*_{weff}\,dx^* = 4.54310^5\ \text{dyn/cm}^2$$

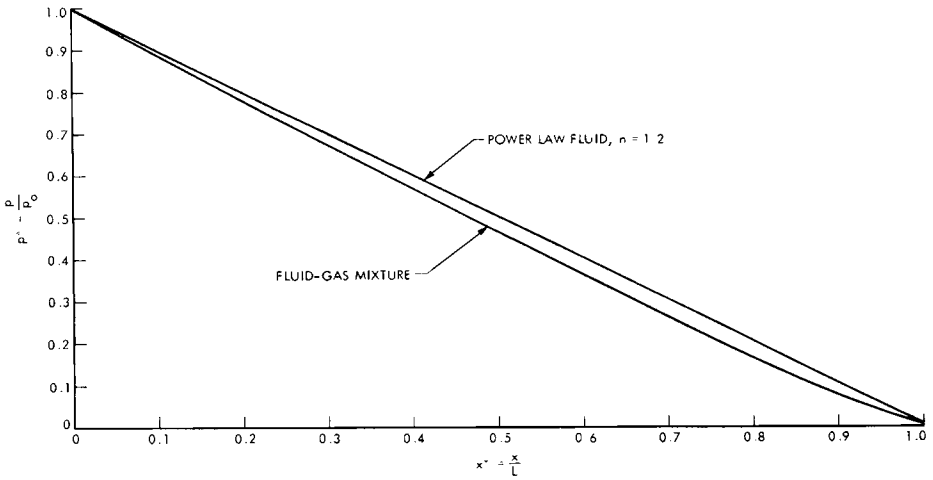

Fig. 2. p^* vs. x^*.

DISCUSSION

The axial-pressure profile shows deviations from the familiar "straight-line" pressure drop associated with the flow of a non-Newtonian power-law fluid. Figure 2 shows that the pressure is less than in a non-Newtonian pipe flow except at $x^* = 0$ and 1. In fact, $p^* = 0.4660$ at $x^* = 0.5$, compared to the pipe flow value of $p^* = 0.505$.

The dimensionless density (Fig. 4) and dimensionless velocity (Fig. 3) show relatively little deviation from their corresponding behavior in non-Newtonian

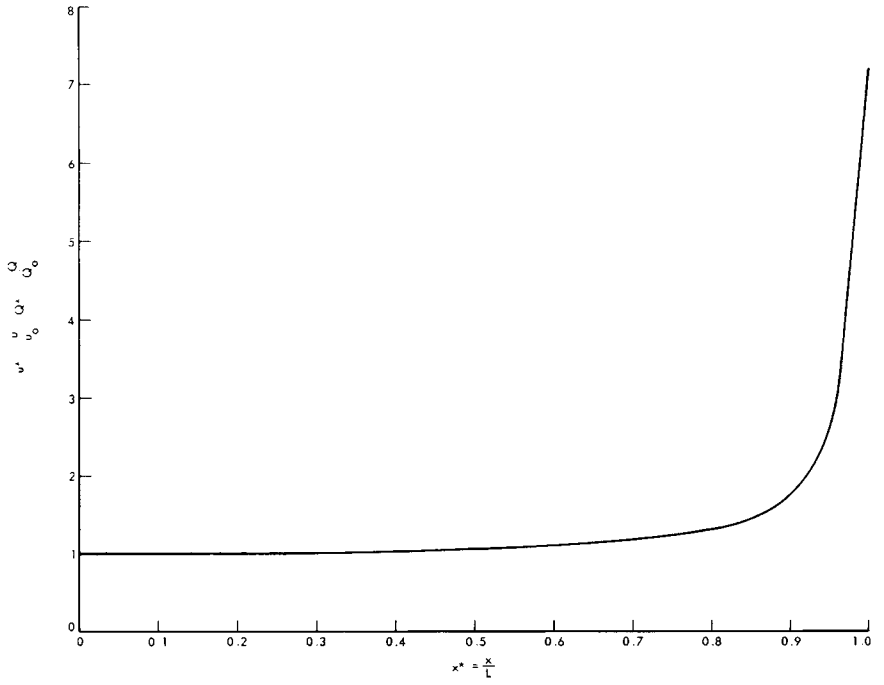

Fig. 3. u^* vs. x^*; Q^* vs. x^*.

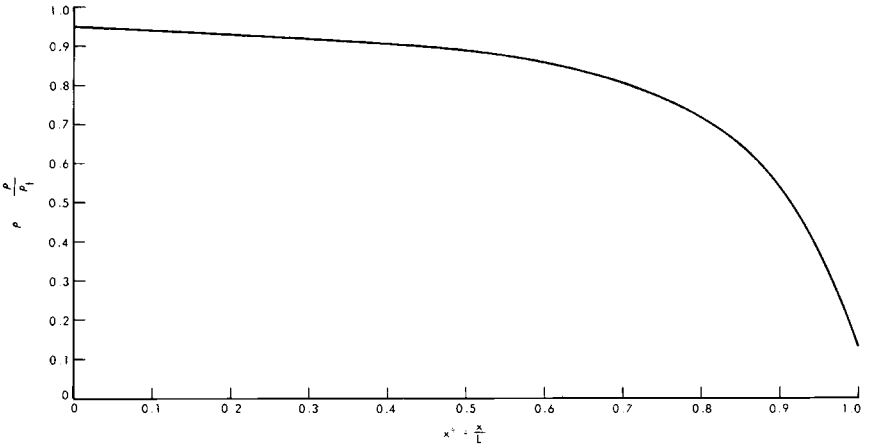

Fig. 4. ρ^* vs. x^*

pipe flow over most of the tube length. The density, ρ^*, is within 10% of its reservoir value, $\rho_0{}^*$, up to $x^* = 0.6$; from $x^* = 0.6$ to 1, a rapid density decrease is observed until the value of $\rho^* = 0.1306$ is reached at $x^* = 1$. The velocity u^* is also within 11% of its reservoir value up to $x^* = 0.6$ and from $x^* = 0.6$–1 a rapid increase is observed until $u^* = 7.213$ is reached at $x^* = 1$. In contrast, $\rho^* = u^* = 1$ for pipe flow of a non-Newtonian power-law fluid over the entire tube length. The rapid density decrease near the tube exit for the fluid–gas mixture can be explained by examining the fluid–gas equation-of-state, eq. (1). Near $x^* = 0$, $p^* \gg p^*_r$ and $\rho^* \simeq (1 + r)$, but near $x^* = 1$, $p^* \ll p^*_r$, and $\rho^* \simeq (1 + r)p^*/p^*_r$.

The dimensionless effective wall shear stress, $\tau^*_{w\text{eff}}$, (Fig. 5) shows a continuously decreasing behavior, decreasing rapidly near $x^* = 1$ where $\tau^*_{w\text{eff}} = 0.3724$. These small values of shear stress act over small tube lengths, however.

The importance of the inertia terms in this problem will now be examined. This comparison is represented by the ratio of the second and last terms in eq. (7) which compares the viscous term to the inertia term. Forming this ratio and substituting numerical values yields:

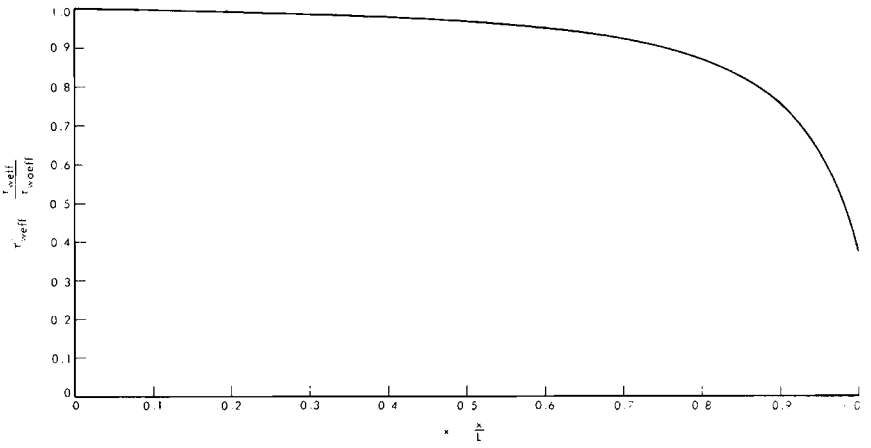

Fig. 5. $\tau^*_{w\text{eff}}$ vs. x^*.

$$\frac{\text{inertia}}{\text{viscous}} = \frac{(GR)^{3/2}p_r^*(p_r^* + p^*)^{1/2}}{2mL[5(1+r)\rho_f]^{1/2}p^{*5/2}}\frac{dp^*}{dx^*} \simeq 6.710^{-7} \ll 1$$

which validates the inertia-free assumption made previously.

With these results we can now compute the apparent viscosity of the fluid–gas mixture. The usual definition for non-Newtonian fluids is $\eta = \tau/\dot{\gamma}$, where τ is the wall shear stress and $\dot{\gamma}$ the shear rate. However, both these parameters vary with axial position in this problem. To be consistent with viscosity measurements made on current experimental equipment (such as the McKelvey–Sieglaff rheometer), we interpret τ to be the length-averaged, effective wall shear stress, $\bar{\tau}_{w\text{eff}}$, and $\dot{\gamma}$ to be the shear rate at $x = 0$. To evaluate $\dot{\gamma}$ we use the expression $\dot{\gamma}_0 = (\tau_{w0\text{eff}}/m)^2$, which assumes the flow profile is locally a power law with $n = \frac{1}{2}$. In fact this may not be true, the actual velocity profile may exhibit other power-law behavior but, without resorting to a two-dimensional analysis, we cannot solve for the exact radial dependence of velocity. Computing the apparent viscosity yields

$$\eta_{\text{app}} = \frac{\bar{\tau}_{w\text{eff}}}{\dot{\gamma}_0} = \frac{\tau_{w0\text{eff}}}{(\tau_{w0\text{eff}}/m)^2}\int_0^1 \tau^*_{w\text{eff}}\,dx^* = \frac{4.543\ 10^5}{47.36} = 9.592\ 10^3\ \text{g/cm sec}$$

The viscosity of the fluid alone corresponds to the flow with the same overall pressure drop but with a different shear rate. The length-averaged, wall shear stress, $\bar{\tau}_w$, shear rate at $x = 0$, $\dot{\gamma}_0$, and resulting fluid viscosity η_f are

$$\bar{\tau}_w = (p_0 - p_a)R/2L = 4.545\ 10^5\ \text{dyn/cm}^2$$

$$\dot{\gamma}_0 = 39.6\ \text{sec}^{-1}$$

$$\eta_f = 4.545\ 10^5/39.6 = 1.148\ 10^4\ \text{g/cm sec}$$

Thus, the fluid–gas mixture represents a reduction in apparent viscosity, since

$$\eta_{\text{app}}/\eta_f = 0.836$$

Blyler and Kwei[1] present evidence that the apparent viscosity of a non-Newtonian fluid decreases with the addition of small weight percentages of gas. They report a 22% reduction in apparent viscosity when 0.5 wt % blowing agent was added to a LDPE. The apparent viscosity was defined by Blyler and Kwei as the ratio of length-averaged, wall shear stress, $\tau_w = \Delta pR/2L$, and apparent shear rate, $\dot{\gamma}_{\text{app}} = 4Q/\pi R^3$, based on capillary entrance conditions (neglecting and effects and polymer compressibility).

The constants used in our model were chosen to correspond to the experimental conditions reported by Blyler and Kwei and, on that basis, the model predicts a 16.4% reduction in apparent viscosity compared with a 22% reduction reported by Blyler and Kwei. The calculation presented here is a one-point comparison (i.e., at one reservoir pressure); however, we feel that the physical model presented here is capable of explaining the observed decrease in apparent viscosity of a fluid–gas mixture compared to the viscosity of the fluid alone.

For simple extrusion channel geometries (i.e., those in which the approximation of one-dimensional flow is adequate), this model can be used to compute the mass flow rate. The fluid properties, gas content, channel dimensions, pressures, and fluid temperature are required. Alternatively, if the mass flow rate is measured, the parameters m and n, in the power-law expression for the fluid, can be ex-

tracted. Equation (7) serves as a starting point for design in the extrusion of plastic foams.

CONCLUSIONS

Based on the results and discussion presented we can draw the following conclusions:

(1) The physical model presented here is capable of explaining the experimentally observed decrease in apparent viscosity when small weight percentages of gas are added to a fluid under flow conditions similar to those found in a capillary rheometer.

(2) The apparent viscosity defined as $\eta_{app}(x) = \tau_{weff}(x)/\dot{\gamma}(x)$ is a function of axial position for flows of fluid–gas mixtures.

(3) The axial pressure, velocity, density, volumetric flow rate, and shear stress profiles of the fluid–gas mixture show departures compared to the corresponding profiles observed in flows of non-Newtonian power-law fluids.

This paper presents the results of research carried out at the Jet Propulsion Laboratory, California Institute of Technology, under NASA Contract NAS 7-100.

References

1. L. L. Blyler and T. K. Kwei, *J. Polym. Sci. Part C*, **35**, 165 (1971).
2. C. D. Han, Y. W. Kim, and K. D. Malhorta, *J. Appl. Polym. Sci.*, **20**, 1583 (1976).
3. C. D. Han and C. A. Villamizar, *Polym. Sci. Eng.*, **18**, 687 (1978).
4. R. B. Bird, W. E. Stewart, and E. N. Lightfoot, *Transport Phenomena*, Wiley, New York, 1960, pp. 180–190.
5. R. B. Bird, R. C. Armstrong, and O. Hassager, "*Dynamics of Polymeric Fluids*," in *Fluid Mechanics, Vol. 1*, Wiley, New York, 1977, pp. 179–220.
6. A. B. Metzner, and J. C. Reed, *AIChE J.*, **1**, 434 (1955).

Received October 3, 1979
Revised March 18, 1980